https://doi.org/10.5194/egusphere-2026-3835
Preprint. Discussion started: 14 July 2026

High temporal resolution in-situ measurement of CO_2 fluxes through Arctic shrub-tundra snowpacks

Victoria R. Dutch[1,2], Nick Rutter[1], Muhammad Waqas Khan[3], Alex Mavrovic[4], Alexandre Roy[5], Sevi Modestou[1], Oliver Sonnentag[6], Carolina Voigt[7,8], Philip Marsh[9], and Paul J. Mann[1]

[1]School of Geography and Natural Sciences, Northumbria University, Newcastle upon Tyne, UK
[2]Department of Earth Sciences, University of Oxford, Oxford, UK
[3]School of Engineering, Physics and Mathematics, Northumbria University, Newcastle upon Tyne, UK
[4] Cégep Sherbrooke, Sherbrooke, Québec, Canada
[5]Département des sciences de l'Environnement, Université du Québec à Trois-Rivières, Trois-Rivières, Québec, Canada
[6]Université de Montréal, Montréal, Québec, Canada
[7]Alfred Wegener Institute Helmholtz Centre for Polar and Marine Research, Potsdam, Germany
[8]University of Hamburg, Hamburg, Germany
[9]Wilfrid Laurier University, Ontario, Canada

Correspondence to: Victoria Dutch (victoria.dutch@earth.ox.ac.uk)

Abstract

Wintertime carbon dioxide (CO_2) emissions from tundra soils likely make a sizable contribution to terrestrial annual Arctic carbon budgets. However, poor availability of wintertime CO_2 flux measurements limits current capacity to quantify the magnitude and variability of non-growing season carbon emissions from Arctic soils, and identify key environmental drivers of CO_2 production and release. To address this, low-cost CO_2 logging systems were developed and deployed in snowpacks at Trail Valley Creek, NT, Canada during late winter periods in 2021-2022 and 2022-2023. CO_2 fluxes calculated from sub-hourly gradients in CO_2 concentrations demonstrated consistent positive (ground-to-atmosphere) emissions, with median flux rates of 0.03 to 0.35 g C m^{-2} d^{-1}, across a range of vegetation types (shrub, tree, tussock) and snow depths (34-136 cm). Stable carbon isotope ($\delta^{13}C$-CO_2) analyses confirmed isotopic enrichment of CO_2 at the base of the snowpack originating from soil emission, and that snowpack gases mixed sequentially with atmospheric CO_2 as they travelled through upper snow layers. Snowpack CO_2 concentration gradients and resultant fluxes were impacted by seasonal increases in air and soil temperatures, especially as near-ground gas temperatures approached the zero-curtain (0ºC) threshold during the winter-spring transition. Positive relationships between CO_2 flux and warming subnivean temperatures across the study site were similar in magnitude to those observed in pan-Arctic winter syntheses. Our results highlight that low-cost sensors may provide a robust and scalable method for monitoring the spatial variability of in-situ winter CO_2 fluxes through snow at high temporal resolution and provide unique insights into winter carbon processes.

https://doi.org/10.5194/egusphere-2026-3835
Preprint. Discussion started: 14 July 2026

1. Introduction

Arctic and sub-Arctic regions store more than half the soil organic carbon on Earth, predominantly within permafrost (i.e. continuously frozen ground; Boike et al., 2023; Schuur et al., 2015). Permafrost thaw could contribute an additional 67 to 237 billion metric tons of carbon to the atmosphere by 2100 (Schuur et al., 2022) due to amplified Arctic warming (Box et al., 2019; Previdi et al., 2021; Yamanouchi and Takata, 2020). While in recent decades the Arctic has warmed up to four times faster than the global average (Rantanen et al., 2022), mean seasonal warming is most pronounced in winter (Giesse et al., 2024). Wintertime carbon emissions will increasingly contribute to annual Arctic carbon budgets (Bruhwiler et al., 2021; Euskirchen et al., 2012; Fahnestock et al., 1998, 1999; Oechel et al., 2014; Welker et al., 2000), with terrestrial cold season emissions projected to increase under future warming (Rafat et al., 2021; Webb et al., 2016), potentially offsetting growing season carbon uptake across the permafrost region (Euskirchen et al., 2016; Natali et al., 2019).

Existing winter measurements of carbon fluxes in snow-covered Arctic environments are highly spatially and temporally limited (Arndt et al., 2023; Mavrovic et al., 2023; Virkkala et al., 2022), with often considerable variability between existing measurement techniques (Björkman et al., 2010; Rains et al., 2016). Despite dissimilar methodological approaches creating variability in the magnitude of CO_2 fluxes (e.g. Celis et al., 2017), it is often necessary to aggregate fluxes across a range of measurement techniques to estimate winter CO_2 emissions across the circumpolar Arctic (Natali et al., 2019). Measurement of fluxes using chambers suffer from snow burial, pressure effects and freezing of external moving parts (Arndt et al., 2023; Virkkala et al., 2018) as well as perturbing the snow thermal regime, making eddy covariance (EC), mounted on towers with no external moving parts, more suitable for winter measurements. Open-path EC is appropriate for remote measurements reliant on battery power and low maintenance requirements, but can be subject to increased data loss especially in harsh meteorological conditions, e.g. winter precipitation and icing of sensors (Arndt et al., 2023; Goodrich et al., 2016), with high measurement noise relative to seasonally low carbon fluxes. Closed-path EC substantially reduces data loss, but requires higher power and maintenance demands which are challenging to meet in remote environments (Hanis et al., 2013). In addition, both open- and closed-path EC measurement methods can be subject to high uncertainties as flux magnitudes are low and rely on empirical corrections, which often do not strictly satisfy underpinning atmospheric stability assumptions (Jentzsch et al., 2021a, b; Webb et al., 1980). Consequently, continuous wintertime measurements are only made at a handful of sites across the Arctic (e.g., Pallandt et al., 2021).

EC footprints aggregate fluxes across surfaces 10 - 100 m^2 in extent, which obscures localised CO_2 emission processes (e.g. Pirk et al., 2017) that have non-linear responses to changes in the surrounding environment, particularly changes in soil temperature and moisture conditions. Although localised emissions in Arctic environments are now beginning to be statistically disaggregated and upscaled within EC footprints (Pirk et al., 2024), CO_2 flux measurements within snow-covered EC footprints are not always in agreement with EC tower fluxes (e.g. Kade et al., 2012), suggesting finer-scale data are required to account for sub-footprint heterogeneity in emission processes. Measurements of vertical CO_2 concentration profiles in snow (Mavrovic et al., 2023; Seok et al., 2009), used to calculate fluxes using the diffusion gradient method (Sommerfeld et al., 1993), offer the potential to isolate spatially heterogeneous emission processes from footprint-scale aggregation and address this measurement gap. However, snapshots in time of vertical CO_2 concentration profiles do not account for any temporal fluctuations in CO_2 emission, either due to temperature and moisture controls on soil respiration rates (Mavrovic et al., 2023) or due to wind pumping within the snowpack (Graham and Risk, 2018; Seok et al., 2009). Recent advances in low-cost non-dispersive infrared (NDIR) CO_2 sensor technology provide a cost and labour-efficient alternative to traditional measurements, such as manual snowpack gas sampling or soda-lime based chambers (Bastviken et al., 2015; Thanh Duc et al., 2020), but have yet to be tested in winter snow environments.

https://doi.org/10.5194/egusphere-2026-3835
Preprint. Discussion started: 14 July 2026

Untangling source contributions is also useful for understanding processes controlling CO_2 fluxes. Although soil respiration provides the most obvious source of subnivean CO_2, processes such as wind pumping (e.g. Colbeck, 1997) may suggest subnivean CO_2 as being sourced from the atmosphere. Soil respiration has a considerably more negative isotopic signature to background atmospheric CO_2 (Tu and Dawson, 2005), and thus stable carbon isotope analysis allows the relative contribution of atmospheric or soil derived endmembers to be estimated.

Here we examine the potential for low-cost CO_2 sensors to:

1. Quantify temporal variability in CO_2 fluxes through snowpacks across contrasting vegetation, snowpack depths and soil types
2. Assess the development of CO_2 concentration gradients within snowpacks and their response to short-term disturbances such as wind-pumping using concurrent measurements of CO_2 concentrations, fluxes and stable carbon isotopes ($\delta^{13}C$-CO_2)
3. Investigate the timing and magnitude of CO_2 fluxes in response to seasonal warming and the onset of snowmelt

2. Methods

2.1: Fabrication and Deployment of low-cost CO_2 logging systems

Low-cost (~ €250) CO_2 concentration logging systems were developed after Bastviken et al., (2015), with modifications to provide a headspace for snowpack gas diffusion and to reduce power requirements. Modifications were progressively made across two field campaigns, resulting in two sensor designs: version 1 (2022) and version 2 (2023). Version 1 used a widely commercially available Sensirion SCD30 NDIR CO_2 sensor (Sensirion AG, Stäfa, Switzerland), with simple to implement Arduino libraries and integration (e.g. I2C communications), and built-in temperature and relative humidity sensors. Sensirion SCD30 sensors were soldered to an Arduino Uno R3 shield (Arduino, Ivrea, Italy) alongside an SD card reader and real-time clock, mounted on an Arduino Uno (R3) for unsupervised data collection logging (Figure 1a). The Arduino and sensor shield were powered using alkaline 6 D-Cell batteries (9V) and housed in a watertight plastic box with dimensions 230 x 300 x 85 mm (Figure 1a & b). Boxes were pale in colour to reduce the potential for radiative heating below the snow surface (Lundberg et al., 2016). Ten 2 cm diameter holes were drilled in the lid of each box, and covered by a waterproof gas-permeable membrane (Polyflon Technology Limited, Stafford, UK) to maintain an equilibration between gases within the snowpack and the box. The membrane was held in place using epoxy glue and rubberised paint (Plasti-Dip UK, Hampshire, UK). Desiccant bags were added inside boxes to reduce condensation and limit potential for water damage to electronics (Bastviken et al., 2015).

Version 2 incorporated the ELG K33 NDIR CO_2 sensor (Senseair AB, Delsbo, Sweden) to reduce power demand, and added an external temperature and humidity sensor (DHT 22; Figure 1c) to provide independent measurements of air conditions (instead of the internal measurements used for sensor corrections). The sensor board was mounted within a small plastic box with dimensions 100 x 65 x 40 mm to create a smaller self-contained headspace than version 1 to improve rates of gas equilibration with external snowpack gases and to separate the Arduino from ongoing exposure to high humidities (Figure 1c). Gases permeated through two 2 cm diameter holes (Figure 1d), covered with the same membrane as version 1, connecting the internal headspace to gases within the snowpack. Solar charging units (DFRobot, DFR0580) were used to trickle charge sealed lead-acid batteries (12V, 7Ah) with a small (25 x 20 cm, 5W) solar panel mounted on vertical wooden stakes above the estimated maximum snowpack height. Battery recharge allowed for substantially longer measurement duration (Table 1) and greater environmental sustainability. In addition, Arduino power use was reduced by incorporation of a timer breakout (Adafruit TPL5110), and the sampling frequency of CO_2 concentration measurements was reduced from 1 min (version 1) to 10 min (version 2) to reduce power draw, thereby collectively extending the measurement period from days to weeks (Table 1).

Calibration of CO_2 sensors (version 1) was performed using an infrared gas analyser (UGGA; Los Gatos Research, San Jose, California) in an air-tight Perspex chamber containing standard calibration gases (399 ppm; LindeCanada, Edmonton, Alberta). All sensors sampled CO_2 every 10 s for 1 hour. The offset between the mean measured UGGA concentration and sensor concentration were then calculated and applied as a single-point correction. The Sensirion SCD30 sensor is specified to an accuracy of ±30ppm (± 3% of absolute range) and precision of ±10ppm. Initial chamber calibrations suggested significant offsets in initial CO_2 concentrations relative to the standard (±200 ppm), but within or near specification once baseline corrected to a single point (± 13 to 33 ppm). Residual scatter suggested instantaneous precision of 10 to 20 ppm for single measurements, yet likely single digit (2 to 5 ppm) after 30-minute aggregation (30 measurements).

Calibration of version 2 CO_2 sensors used an alternative field ready approach. Initial laboratory testing demonstrated that the Senseair K33 sensors similarly had significant offsets in CO_2 accuracy direct from manufacture (ranging from -102 to +118 ppm) and that these offsets were relatively stable and systematic over environmentally relevant concentrations (400 to 900 ppm). To account for these offsets under realistic conditions, both sensors were left to measure simultaneously on the snow surface prior to burial (ca. 60 minutes), and the offset between these two concentrations applied as a single fixed correction to the upper sensor (avoiding the need for calibration gases in remote deployments). The K33-based systems exhibited excellent instantaneous precision and low noise (1.4 to 1.7 ppm), with estimated 30-minute precision of 0.87 to 1.15 ppm (3 measurements). Both the SDC30 and K33 sensors automatically corrected for temperature effects (including self-warming) using manufacturers built-in compensation. No additional temperature or pressure corrections were applied.
Prior to initial deployment, field tests showed sensors took less than 12 hours to equilibrate to ambient temperature, humidity and CO_2 concentration within the snowpack after deployment. Sensor pairs were discounted if calibrated measurements gave consistent CO_2 concentrations lower than 400 ppm for either sensor, which was found at one site in the first field campaign. Additionally, sensors at an additional microsite were discarded due to the presence of an ice lens in the upper part of the snowpack (as noted during snow density characterisation) causing recirculation of air within the snowpack, thereby invalidating assumptions of Fick's second law of diffusion during the flux calculation.

2.2: Site Characterisation and Sensor Deployment

Measurements of CO_2 concentration were undertaken at Trail Valley Creek (TVC; 68°45'N, 133°30'W), a 57 km^2 forest-tundra ecotone research watershed located in the Inuvialuit Settlement Region, approximately 55 km north-east of Inuvik, NT, Canada. Ground cover at TVC consists mainly of mineral upland tundra, with shrub patches, tussocks, small lakes, and isolated spruce stands (Grünberg and Boike, 2019) (Figure 2). The site has continuous permafrost to a depth of 350 - 500 m (Wilcox et al., 2019), with a maximum seasonally unfrozen active layer reaching depths of up to 1 m at the end of the summer (Grünberg et al., 2020). The TVC meteorological station (Tutton et al., 2026; for location see Figure 2) provided half-hourly 2 m air temperatures (HMP35CF sensor, Campbell Scientific, Logan, Utah) and wind speed (05103-10 wind monitor, R.M. Young, Traverse City, Michigan).

Logger deployment microsites across the wider TVC site were selected to cover a range of different vegetation types (Figure 2) which act as a proxy for different soil properties, hydrological and micro-meteorological conditions (including active layer depth). Within vegetation types, specific microsite locations were informed by point measurements of wintertime CO_2 fluxes from Mavrovic et al. (2023), in order to maximise the potential range of measured fluxes whilst targeting microsites where fluxes were likely to be larger than instrumental error. Snow depth transects characterising the statistical distribution of snow depth in the study area (~1000 depth measurements over 1 km transects) were used to refine exact sampling locations to be representative of snow depth variability within vegetation types for sensor deployment and isotopic measurements. At each microsite (Figure 2), measurements were made of total snow depth plus vertical profiles of snow stratigraphy, density, and temperature (after Fierz et al., 2009) immediately prior to sensor deployment in late March. In 2022, snow density profiles were made at a 3 cm vertical resolution using a 100 cm^3 box cutter (Conger and McClung, 2009). In 2023, Snow

https://doi.org/10.5194/egusphere-2026-3835
Preprint. Discussion started: 14 July 2026

MicroPenetrometer (SMP; Proksch et al., 2015) force profiles were used to derive snow densities using parameters described by Dutch et al., (2022). Porosity and tortuosity were estimated from measured snow densities at each microsite using Equations 3 and 4. Finally, pairs of low-cost logging systems were inserted into the face of each snowpit in carefully excavated holes in the snowpit wall (Figure 1e) and their relative heights within vertical profiles were noted. The lower sensor was as close to the snow: ground interface as possible (not always possible due to the presence of shrubs) and the upper sensor was located in the upper part of the wind slab layer. Snowpits were then immediately backfilled with snow, and sensor measurements were only considered after 12 hours, once CO_2 equilibrium conditions had returned to the snowpack profile.

2.3: Calculating CO_2 Flux

Diffusive fluxes (F_{CO2}) of CO_2 were calculated from concentration differences between the top and bottom of the snowpack as per Seok et al. (2009) & Sommerfeld et al. (1993):

$$F_{co_2} = \varphi t D_{CO_2} \Delta CO_2 \tag{1}$$

where ΔCO_2 is equal to the difference in CO_2 concentration between upper and lower sensors within the snowpack, D_{CO2} equals the diffusivity of CO_2 and φ and t represent the porosity and tortuosity of the snowpack respectively. Snow density, porosity and tortuosity was considered constant throughout the duration of the sensor deployments. D_{CO2} is calculated as a function of temperature (Air - Diffusion Coefficients of Gases in Excess of Air, 2023):

$$D_{CO_2} = \frac{(0.000001T^2 + 0.001T + 0.139)}{10000} \tag{2}$$

where T (in °C) is the mean temperature of gas towards the base of the snowpit. Snow tortuosity (t) was estimated from the porosity (φ) of the snowpack:

$$t = 1 - (1 - \varphi)^{\frac{2}{3}} \tag{3}$$

with φ in turn estimated from the snow density (ρ_{snow}) and the density of ice (ρ_{ice}):

$$\varphi = 1 - \frac{\rho_{snow}}{\rho_{ice}} \tag{4}$$

after Filippa et al. (2009). A value of 917 kg m^{-3} was used for the density of ice, where identified in the stratigraphic profiles, or for the tortuosity calculation. As air temperatures were well below freezing, all snow was dry at the time of sensor installation and assumed to stay dry for the duration of the measurements.

2.4: Isotopic Gas Measurements and Bayesian Mixing Model

To identify the relative contributions of soil and atmospheric sources to CO_2 within the snowpack, we measured the stable isotopic composition of CO_2 ($\delta^{13}C$-CO_2, henceforth $\delta^{13}C$). Stable carbon isotopes have been used to examine net CO_2 exchange across a variety of landscapes (Ehleringer et al., 2002; Tu and Dawson, 2005; Zhu et al., 2019), and from incubations in frozen tundra soils (Pedron et al., 2023), but rarely in snowpacks (though see Bowling et al., 2009). Vertical profiles of CO_2 and $\delta^{13}C$ were collected at all four 2022 microsites, plus 5 additional locations close to the TVC meteorological tower (CA-TVC in the AmeriFlux network, Graveline et al., 2024; Figure 2 - grey dots). Additionally, CO_2 and $\delta^{13}C$ profiles were collected daily for six days (22 - 27 March 2022; between 11:00 and 20:00 local time) at a location approximately 50 m north of the TVC tower to examine the temporal variability in snowpack CO_2 provenance over time. Atmospheric air samples were also collected at 3 heights above the snow surface (0.5, 1 and 1.5 m), in order to provide an end member for the isotope ratio mixing model. Samples were collected using 60 ml gas-tight syringes (plastic with butyl rubber) connected via a 3-way stopcock to a graduated hollow steel rod inserted vertically from the surface into the snowpack. Two 60 ml syringe samples were taken at each of four depths (just below the snow surface, in the middle of both the wind slab and depth hoar layers and at the base of

https://doi.org/10.5194/egusphere-2026-3835
Preprint. Discussion started: 14 July 2026

the snowpack) within the snowpack stratigraphy using the steel rod, and two samples were collected just above the snowpack surface to capture the snow-atmosphere boundary (see Appendix A). For each depth, gas in the first syringe was analysed for CO_2 concentrations using an infrared CO_2 and H_2O gas analyser (Li-COR LI-850; Li-COR Environmental, Lincoln, Nebraska). Gas from the second syringe was injected into pre-evacuated exetainer vials (Labco Ltd, Lampeter, UK) with a double-wadded septum for laboratory analysis of $\delta^{13}C$. These 12ml vials were over-pressured with approximately 25 ml of sample (at atmospheric pressure) to minimise the likelihood of atmospheric contamination and to increase the sample amount for later laboratory analysis.

Details of the isotopic method and information required to conform with data standards for isotope geochemistry as laid out by Skrzypek et al., (2022), including the uncertainty of $\delta^{13}C$ ratios, are as follows. Two in-house gas standards for isotope measurement were prepared by evolving CO_2 from in-house carbonate standards ('Plessen' [marble calcite], and 'Pol2' [speleothem calcite]; >1.95 g/ml phosphoric acid). Evolved CO_2 was cryogenically purified on a manual vacuum line with three passes through a -90ºC slush trap (Godwin Laboratory, Cambridge University, UK) and then diluted with 'zero air' (air mix with CO_2 removed, BOC Ltd) to produce gas mixtures with comparable concentrations to snowpack gas samples. Three commercially available air-like mixtures with certified CO_2 concentrations of 310, 640, and 1022 +/- 10 ppm (balance zero air; BOC Ltd) were used to estimate concentration, and alongside the in-house gas mixtures, monitor linearity, drift, and instrument performance. $\delta^{13}C$ and CO_2 concentrations were measured using a Thermo Fisher Gasbench II coupled to a Delta V isotope ratio mass spectrometer (IRMS) via a Conflo IV, with the GasBench II GC oven temperature set to 50 ºC. Timed dilution was used to 'blank' gases other than CO_2 after Levitt (2014); dilution was timed to stop two and a half seconds before CO_2 peaks to minimize fractionation. This strategy removed the majority of undesired gases eluting prior to CO_2. The IRMS method was otherwise identical to standard continuous flow-IRMS methods used for measurement of solid carbonate samples, e.g. Spötl and Vennemann (2003), with normalization of in-house gas standards and supplied gas mixtures following Kim et al. (2015) using at least four each of NBS18 and NBS19 in a set of initial calibration runs. Initial data correction steps were performed in Isodat (ThermoFisher Scientific), with working gas compositions determined also via normalization to NBS18 and NBS19. The in-house gas mixtures were used to normalize samples on a per measurement sequence basis, where at least 5 of each of the supplied and in-house prepared gas mixtures were measured alongside samples. Linearity and drift corrections were not applied, as these did not improve precision. Separate aliquots of in-house Pol2 gas standard (the most similar to sample isotopic composition), were used as a monitor standard to check for internal consistency and assess the quality of the normalization procedure. Over the course of all runs, the average $\delta^{13}C$-CO_2 value of the Pol2 gas mixture was -6.9 ‰ (n = 45, σ = 0.4 ‰; all $\delta^{13}C$ values in this paper are given in VPDB). Uncertainty per measurement sequence was calculated as the standard deviation of corrected $\delta^{13}C$ values for all samples of in-house standards in each run, with a maximum value of 0.49‰. CO_2 concentrations were estimated using a linear regression through the results of the three supplied gas mixtures, also calculated on a per run basis; CO_2 concentration uncertainty was typically less than 5 ppm (< 1%), with a maximum of 15 ppm (2.7%) for some measurements.

The R package MIXSIAR (v3.1.12; Stock et al., 2018) was used to develop a Bayesian tracer-mixing model to estimate atmospheric and soil source contributions. Air samples collected from above the snow surface (at 0.5 to 1 m height) were combined to calculate the mean and standard deviation in the atmospheric CO_2 endmember (-10.7 ± 1.1, n = 20). Soil endmembers were determined from measurements of $\delta^{13}C$ in bulk soils from TVC (-26.3 ± 0.6, n = 54) covering a range of organic, mineral and mixed transitional soils and permafrost (Voight, Pers Comm). To account for $\delta^{13}C$ bulk soil OM fractionation into respired CO_2 we allow a discrimination factor of +2 ± 1 ‰ (Boström et al., 2007; Nickerson and Risk, 2009). To evaluate the relative importance of environmental controls on CO_2 concentrations, we compared four models; 1) Null (no explanatory structure), 2) snow depth as a continuous covariate, 3) plant functional type as a random effect, and 4) both snow depth and plant functional type simultaneously. All Markov chain Monte Carlo models runs used a chain length 1,000,000

https://doi.org/10.5194/egusphere-2026-3835
Preprint. Discussion started: 14 July 2026

iterations, and performance was compared using leave one out information criterion scores (LOOIC; MixSIAR GUI User Manual. Version 3.1).

3. Results

3.1: CO_2 Flux and Provenance in Winter Snowpacks

Median CO_2 fluxes measured across all microsites and measurement periods indicate consistently positive emissions from soil to the atmosphere, ranging from 0.03 to 0.35 g C m^{-2} day^{-1} (Figure 3). The inter-quartile range (IQR) of CO_2 fluxes are similar at all microsites except for the sparsely forested microsite (TRE), which displayed statistically higher emissions (Kruskal-Wallis ANOVA; $p < 0.0001$).

Soil-derived CO_2 had a greater influence on the isotopic composition of higher CO_2 concentrations within snowpacks. Stable carbon isotope ratios showed a statistically significant negative linear relationship and high model fit (R^2 = 0.84, $p <$ 0.0001) with CO_2 concentrations (Figure 44a). More negative δ^{13}C ratios, indicating a greater abundance of soil-derived CO_2 (Tu and Dawson, 2005), were associated with higher CO_2 concentrations that were commonly found towards the base of a snowpack. Consequently, emission of soil-derived CO_2 drives positive CO_2 fluxes through the snowpack towards the atmosphere (R^2 = 0.68, p = 6 x 10^{-4}; Figure 4b), with a reasonable fit between warmer gas temperatures at the lower sensors and increased soil-derived fluxes (R^2 = 0.50, p = 7 x 10^{-4}; Figure 4c). Warmer mean gas temperatures at the lower sensors in 2023 (-10 to -16 °C in 2023 compared to -15 to -20 °C in 2022) were indicative of a longer duration measurement period extending through April and May, incorporating the influence of a seasonally warming atmosphere.

No strong associations were evident between median CO_2 flux magnitudes and snow depth. For example, the highest CO_2 fluxes were found at the forest microsite (TRE) with a snow depth of 120 cm, while low fluxes were evident at shrub microsites (TSH and RSH) with similar snow depths to TRE. However, Bayesian model comparisons indicated strong support for models including snow depth as a continuous covariate, with increasing snow depth leading to an increasing proportion of in soil-derived CO_2. Limited additional explanatory power was provided by the inclusion of PFT in the Bayesian model (Appendix B), suggesting that physical snowpack properties act as the dominant control of source contributions to snowpack CO_2. While CO_2 fluxes are driven by soil emission, CO_2 at the base of the deepest snowpacks was still primarily atmospheric in origin (>75 % atmospheric), with decreasing contributions of soil-derived CO_2 moving toward the surface.

3.2: Wind pumping

Within CO_2 flux distributions, which consisted broadly of positive emissions, occasional negative CO_2 fluxes occurred (Figure 3). Negative fluxes are due to temporary disruption of a monotonically declining CO_2 concentration with increasing distance from soil through the snowpack to the atmosphere. Such a temporary disruption is demonstrated in daily profiles of CO_2 concentrations and δ^{13}C ratios over a sequence of six days at the same microsite (Figure 5), which show inverse relationships between CO_2 concentration and depletion of δ^{13}C (larger negative values) indicative of soil emissions driving CO_2 fluxes. Rising wind speed on 23-24 March from <1 m s^{-1} to a peak of 9.3 m s^{-1} causes dilution of CO_2 concentrations within the snowpack to <460 ppm due to wind-pumping of atmospheric air into the snowpack (e.g. Colbeck 1997, Graham and Risk, 2018). As wind speeds decreased to < 3 m s^{-1} on 25-26 March, vertical profiles of CO_2 concentrations and δ^{13}C profiles returned to patterns more consistent with the re-establishment of a soil CO_2 emission dominated system. During this six-day period, it is likely that wind-pumping temporarily forced atmospheric air with low CO_2 concentrations into lower layers of the snowpack, beneath higher CO_2 concentrations in upper snowpack layers which were previously emitted from soil and diffused vertically through the snowpack. Negative vertical CO_2 concentration gradients during wind-pumping events will lead to calculation of diffusive fluxes inadvertently suggesting CO_2 uptake by soils, rather than emission of CO_2 to the atmosphere. Hence, the small proportion of negative fluxes in statistical distributions of CO_2 fluxes at each microsite (Figure

https://doi.org/10.5194/egusphere-2026-3835
Preprint. Discussion started: 14 July 2026

3), are likely caused by wind-pumping dilution of CO_2 in lower snowpack layers, which will more greatly affect shallower snowpacks covering tussock grasses, or where shrubs create vertical connectivity for air flow through snowpacks.

3.3: CO_2 fluxes over the Winter to Spring transition

Median concentrations of CO_2 at the base of the snowpack increased week-by-week at all three 2023 sites (SHT, SHR, and TSK), concurrent with rising median snowpack gas temperatures. As temperatures rose above -5 °C, the range of basal snowpack CO_2 concentrations increased, leading to greater variability in the exponential relationship. Fluxes of CO_2 also increased in magnitude with increasing lower sensor gas temperatures (Figure 6b), showing a similar exponential pattern as in the synthesis of Natali et al. (2019); 85 % of half-hourly mean flux values from low-power sensors were within the confidence intervals of Natali et al. (2019).

Air temperatures first began to exceed 0 °C for parts of the day from 4 May onwards (Figure 7c and d), and then from 14 May air temperatures more regularly exceeded 0 °C, often for all of each day. Only data prior to this point (i.e. when weekly median lower sensor temperatures were below zero degrees) is shown on the rest of the figures, as flux data during the period of rapid snowmelt denotes a departure from the winter conditions we predominantly discuss. Notable increases in CO_2 fluxes were coincident with the onset of surface snowmelt in 2023 (Figure 7a and b). Prior to 4 May, the shallow (25 cm) snowpack within grass tussocks (TSK) maintained a consistent pattern of positive CO_2 fluxes (mean TSK = 0.08 g C m^{-2} day^{-1}) with a regular but small diurnal amplitude. Over the same period, CO_2 fluxes within a deeper (107 cm) snowpack in shrub/tree vegetation (SHT) exhibited broadly positive fluxes with a less regular diurnal pattern (mean SHT = 0.07 g C m^{-2} day^{-1}). Warmer air temperatures started causing periodic surface melt from 2 May onwards, and caused basal gas snowpack temperatures to first reach 0 °C at the shallow TSK snowpack on 3 May and then 4 days later at SHT on 7 May, due to greater thermal insulation from the deeper snowpack. Intermittent daily melt followed, causing a more erratic pattern in CO_2 fluxes, often peaking at over 2 g C m^{-2} day^{-1} and most likely influenced by snow melt, with changes to snowpack properties influencing gas diffusion and surface meltwater percolation reaching the soil and allowing for greater rates of microbial activity.

4. Discussion

4.1: CO_2 Emissions

Novel application of low-cost CO_2 logging systems within snowpacks shows positive CO_2 fluxes from late-winter frozen tundra soils, which increase exponentially with increasing basal snowpack gas temperatures. Median CO_2 fluxes are similar across tussock and shrub land cover types (0.03 - 0.1 g C m^{-2} day^{-1}), while enhanced emissions from a sparsely forested microsite (0.35 g C m^{-2} day^{-1}) are likely due to greater availability of organic material from plant litter, in combination with deeper snow maintaining warmer winter ground temperatures. The magnitude of CO_2 fluxes from our low-cost systems and their exponential relationship with increasing temperature are consistent with established, often higher precision, measurement methodologies. For example, magnitudes of CO_2 fluxes are similar to fluxes calculated using diffusion gradient methods from syringe-sampled gases at TVC analysed using multiple commercially available CO_2 analysers (Mavrovic et al., 2023), and are similar to a synthesis of pan-Arctic CO_2 fluxes using a wide variety of measurement techniques (Natali et al., 2019), with 85 % of half-hourly mean flux values from our systems within the confidence intervals of Natali et al. (2019). As Natali et al. (2019) compared CO_2 fluxes with soil temperatures at 10 cm average soil depth, and winter soil temperatures are likely to be warmer than the temperatures of gases within snowpacks, consideration of any soil-gas temperature offset would only bring a greater proportion of our CO_2 flux measurements within the Natali et al. (2019) uncertainty bounds. Mavrovic et al. (2023) measured soil temperatures within 1 cm of the ground surface, more similar to basal snowpack temperatures, with their best fit relationship better approximating low-cost system CO_2 fluxes warmer than -10°C, whereas the Natali et al. (2019) best-fit better approximates low-cost sensor CO_2 fluxes colder than -10°C. The exponential increase in CO_2 fluxes measured by our

https://doi.org/10.5194/egusphere-2026-3835
Preprint. Discussion started: 14 July 2026

systems to warming temperatures between -15 and 0 °C is similar to both Mavrovic et al. (2023) and Natali et al. (2019), and would likely be more similar if offsets between different locations of temperature measurements in the snow-soil vertical profile were considered. Consequently, similarities in the magnitude of CO_2 fluxes and their relationship to temperature, demonstrates this novel application of low-cost loggers provides reliable diffusion gradient estimates of CO_2 through snowpacks to the atmosphere.

4.2: CO_2 Fluxes and Scaling

Measured carbon isotope ratios demonstrate that higher CO_2 fluxes are dominated by greater abundance of soil-derived CO_2 and are coincident with higher basal snowpack gas temperatures. However, while soil respiration drives winter CO_2 emissions to the atmosphere, the majority of CO_2 within the snowpack (~75-95 %) is atmospheric in provenance. As Arctic snowpacks are, by total density, approximately two-thirds air (Derksen et al., 2009, 2014) they are well-ventilated to atmospheric CO_2 . Even dense wind slab layers are usually <450 kg m^{-3} (approximately 50 % air), providing low impedance to vertical gas diffusion from the soil or atmosphere, as noted by Hould Gosselin et al. (2025). Accordingly, unless a spatially coherent ice lens of sufficient thickness (formed from a surface melt or rain-on-snow event) traps CO_2 emissions (e.g. Pirk et al., 2016), emissions from soil drive positive CO_2 fluxes to the atmosphere, and the Arctic snowpack itself acts as neither a major store nor producer of CO_2.

Towards the end of the winter, when basal snowpack temperatures were below 0 °C, spatial variability between median CO_2 fluxes across all microsites was low, with the exception of the forested microsite (TRE), where enhanced fluxes were observed. While the sparse spruce forest microsite did not have notably warmer basal snowpack temperatures, there is potential for higher soil organic content from decomposing leaf litter, and low rates of tree root respiration in frozen soils (Du et al., 2013; Muhr et al., 2009; Noguchi et al., 2021) which has previously been shown to enhance soil CO_2 emissions at lower latitudes (Mazzola et al., 2022). At non-forested microsites, variability in sub-zero basal snowpack temperatures was the dominant control over CO_2 fluxes, corroborating relationships previously identified through temporal snapshot measurements at Trail Valley Creek (Mavrovic et al., 2023) and aggregated monthly measurements across the wider pan-Arctic (Natali et al., 2019). However, spatially distributed measurements at high temporal resolution enabled robust comparison of CO_2 flux response rates to meteorological warming and increased soil moisture availability (Mast et al., 1998).

Sub-hourly sampling allows for greatly improved measurement of the non-linear response of microbial respiration to changes in soil temperature and moisture, and better accounts for divergent lag times between microbial respiration of CO_2 in different levels of the soil column and emission to the snowpack. As frozen soils warm to near-zero temperatures at the end of winter, the diurnal amplitude of CO_2 fluxes increases, indicative of the exponentially increasing response of soil respiration to warming. Rapid responses suggest sub-daily lag times between microbial soil respiration and emission to the snowpack from frozen soils, where diffusion is possible through dynamically interconnected micropores (Rooney et al., 2022) . However, where vertical soil porosity is low or impermeable, there is potential for additional delayed release of CO_2 produced in lower soil layers. Macropores created by aperiodic vertical cracking in frozen upper soil layers may provide conduits for gaseous emissions from lower sections of the soil column at warmer sub-zero temperatures or potentially from unfrozen layers between the active layer depth and the descending winter freezing front (Raz-Yaseef et al., 2017; Zona et al., 2016). In addition, as surface snowmelt begins, fast soil microbial responses to the combination of latent heat release when meltwater re-freezes on contact with frozen soil and increased availability of liquid water, causes rapid spikes in CO_2 fluxes. Consequently, only by sampling CO_2 fluxes at a high temporal resolution can aperiodic CO_2 emissions through frozen soil macropores and rapid spiked responses to meltwater be appropriately aggregated with more consistent CO_2 emissions from soil micropore diffusion to account for sub-seasonally variable patterns of emissions. As wintertime precipitation changes as the Arctic warms (e.g. Bintanja and Andry, 2017; Bjerke et al., 2024; Box et al., 2019; Bradley et al., 2025), increasing meltwater availability from winter “rain-on-snow” events (Bintanja and Andry, 2017; Maina and Kumar, 2025) may increase the frequency of aperiodic increases in CO_2 emissions.

https://doi.org/10.5194/egusphere-2026-3835
Preprint. Discussion started: 14 July 2026

Spatial variability of winter-long CO_2 flux budgets is challenging to measure and upscale. While winter CO_2 flux measurements using eddy covariance techniques in Arctic environments can be challenging, especially when restricted to open-path EC systems, their high temporal resolution provides current best estimates of winter CO_2 flux budgets. However, as EC measurements are aggregated across a dynamic footprint varying in dimension and location depending on prevailing meteorological conditions, it is problematic to attribute CO_2 fluxes for an entire EC tower footprint to contributing processes that have small spatiotemporal variability (often on smaller spatial scales than the footprint) and non-linear responses to environmental change. Sufficient distribution of low-cost logging systems across a landscape or EC footprint will help disaggregate competing combinations of physical and biogeochemical processes that influence footprint-scale CO_2 emissions. Spatially refining the physical characterisation of land cover and empirically linking to biogeochemical responses, allows for needed improved understanding of kinetic expressions linking microbial CO_2 production with frozen soil processes (Byun et al., 2021), offering new opportunities for application in terrestrial biosphere models and guiding better understanding of underlying biogeochemical processes. In addition, spatially distributed CO_2 measurements using low-cost logging systems may assist new applications of Bayesian neural networks to disaggregate EC fluxes and processes from different landscape features (Pirk et al., 2024), or support Bayesian kriging approaches to better characterise optimal sampling design and quantify uncertainties when upscaling fluxes from point to landscape scales (Levy et al., 2022). Upscaling can also be undertaken using highly distributed low-cost measurements to refine empirical relationships or add more explicit process representation in terrestrial biosphere models (such as CLM or JULES: Clark et al., 2011; Lawrence et al., 2019) for application over broader spatial extents, albeit with such models usually run at a coarser resolution. Using systems like ours to help parameterise processes with temporal non-linearities could constrain critical parameters that govern winter CO_2 fluxes, thereby addressing significant calibration gaps. Parameterisation of soil respiration as a function of soil temperature (Q_{10}) is a particularly pressing example, as Q_{10} varies latitudinally (e.g. Chen et al., 2020) yet it is poorly parameterised for application in Arctic plant functional types where default model parameterisations are often derived from mid-latitude measurements (Dutch et al., 2024; Tao et al., 2021).

4.3: Future Opportunities

Low-cost CO_2 sensing and logging systems have demonstrated new capacity for month-long measurements of hourly CO_2 fluxes, and ultimately the potential to measure full winters of CO_2 fluxes. In addition, there is potential to add coincident measurements of soil moisture and temperature, as well as snow temperature, to quantify the influence of key variables governing CO_2 flux rates. The low per-unit cost allows for high density spatial distributions of sensing and logging systems at a lower cost than is currently possible with EC tower or chamber measurements. Such low-cost CO_2 logging solutions strongly increase the capacity for sampling across wide gradients of physical and biogeochemical influences controlling winter CO_2 fluxes from Arctic tundra, which is critical for the development of terrestrial biosphere models and may help focus future work on the identification and understanding of underlying biogeochemical processes controlling winter CO_2 fluxes. In particular, the potential for high density sensor deployments creates new opportunities, using a space-for-time approach, to measure contemporary environmental gradients that are analogous to changes expected in a warming Arctic, e.g. multiple densities and heights of shrub development or vegetation recovery from wildfire. In all spatially distributed sensor deployments, hourly resolution measurements over multiple months will be specifically useful for measurement of thermal insulation of soil from early-winter snow accumulation, which is critical for establishing rates at which the zero-curtain descends through the soil column. The zero-curtain is sensitive to the timing, magnitude and phase of early-winter precipitation, when combined with vegetation and topographic controls over wind-redistribution of snow, influencing the spatial heterogeneity in coupling between atmospheric temperatures and soil temperatures until insulation saturation is reached at an effective mean snow depth of ~50 cm (Slater et al., 2017). Consequently, as late winter statistical associations between deeper snowpacks and soil temperatures are usually poor (e.g. $R^2 = 0.035$ in this study), assessment of early-winter snow-soil-carbon flux interrelationships, combined with spatial variations in biogeochemical availability e.g. soil carbon (Lupascu et al.,

https://doi.org/10.5194/egusphere-2026-3835
Preprint. Discussion started: 14 July 2026

2018; Paré and Bedard-Haughn, 2013; Pedron et al., 2022) and nitrogen availability (Christiansen et al., 2012; Schimel et al., 2004), could unlock understanding of variability in winter-long CO_2 flux budgets.

Beyond expanding CO_2 flux measurement networks (e.g. Blackstock et al., 2019; Saccardi et al., 2025), cheaper logging systems have broader social implications, increasing accessibility for future CO_2 flux measurements. Increased measurement capacity can empower citizen scientists, as seen for studies of urban and indoor air quality (Ali et al., 2016; Oyola et al., 2022) and has great potential for scientific engagement, education and outreach, e.g. CO_2 (Pino et al., 2019; Saccardi et al., 2025) and other gases (Reivanth et al., 2024). Increased engagement can enable greater direct community involvement in scientific endeavours, supporting local people in monitoring their environment; such capacity building opportunities are particularly relevant for Indigenous communities living across the Arctic (Johnson et al., 2016). Enabling robust data collection networks by building long-term local capacity through local partners and communities in remote Arctic regions, increases the resilience of measurement networks and offers an opportunity to reduce the carbon footprint and negative environmental impact of Arctic science.

5. Conclusion

Low-cost sensing approaches successfully measured hourly CO_2 fluxes through late winter snowpacks across different vegetation types, land covers, and snow properties at a mineral upland tundra site in the western Canadian Arctic. CO_2 fluxes were broadly positive, indicating CO_2 emissions from soil to the atmosphere across different land covers from late winter to the beginning of snowmelt. Snow properties had a lower impact on the measured CO_2 fluxes than anticipated, with similar fluxes from microsites with differing late winter snow depths. Isotopic analysis confirmed that CO_2 fluxes were derived from soil respiration. Fluxes across the different vegetation covers were typically of a similar magnitude, although higher CO_2 emissions were measured under tree stands – likely due to differences in the soil properties, e.g. temperature, moisture, and nutrient and organic matter availability. Air temperature increases during the winter-spring transition had a greater impact on magnitudes of CO_2 fluxes than short term phenomena such as wind-pumping. CO_2 fluxes measured using low-cost systems showed a similar relationship to subnivean temperatures as measurements synthesised from across the Arctic (Natali et al., 2019).

Our low-cost sensor approach shows potential to improve data coverage and assist with sub-footprint upscaling of eddy covariance measurements for Arctic CO_2 fluxes. Further sensor deployments across a broader range of sites could help improve Arctic data coverage and work towards constraining unknowns and uncertainties in the Arctic carbon budget. Data from such an approach could also be used to help constrain relationships between environmental drivers and wintertime CO_2 flux across a greater range of locations, ultimately feeding into improved representation and parameterisation of Arctic CO_2 fluxes in terrestrial biosphere models.

https://doi.org/10.5194/egusphere-2026-3835
Preprint. Discussion started: 14 July 2026

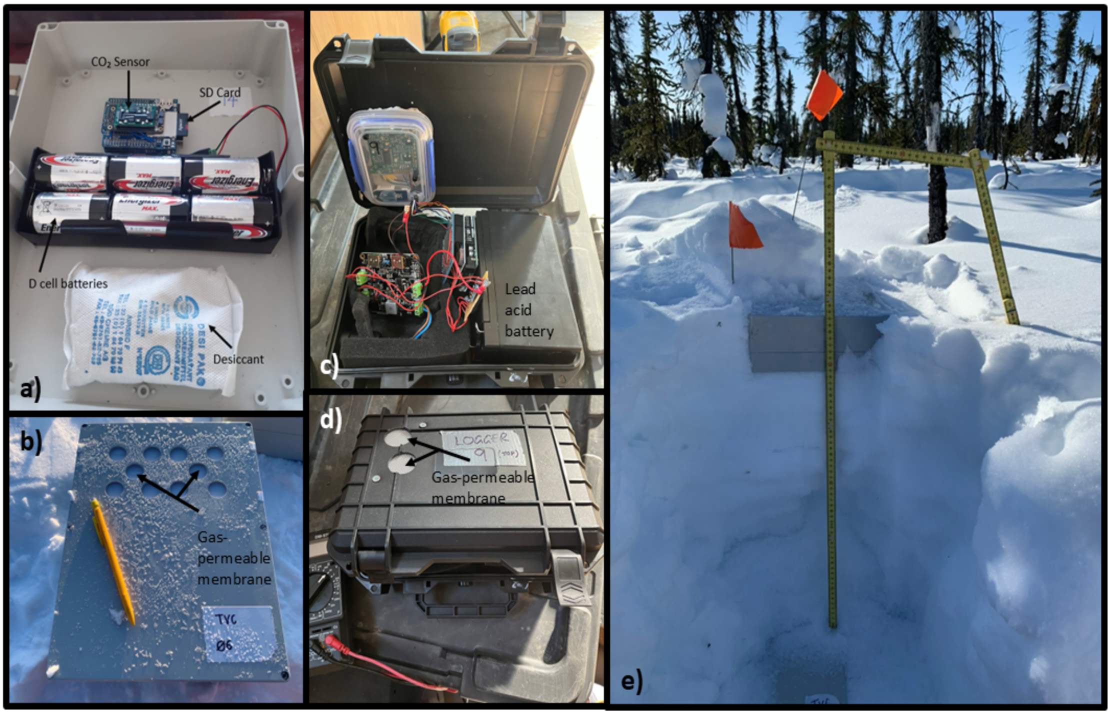

Figure 1: Interior and exterior of the 2022 (a & b) and 2023 (c & d) low-cost CO_2 logging systems. Deployment of the sensors at two vertically aligned positions in the snowpack is illustrated in e) for 2022.

Table 1: Measured snow properties at each sensor microsite and calculated snow porosity and tortuosity. Mean temperature values refer to the mean temperature over the duration of the measurements prior to 1 May. Mean snow density refers to the mean snow density of the vertical profile at the time of sensor deployment.

Microsite name	Vegetation Type	Year	Date of First Measurement	Date of Final Measurement	Data duration [days]	Snow depth [cm]	Lower sensor mean temp (°C)	Mean snow density [kg m^{-3}]	Distance between sensors [cm]	Porosity	Tortuosity
TSH	Tall Shrub	2022	21 Mar	25 Mar	4	110	-20	316	130	0.66	0.51
TRE	Trees	2022	21 Mar	25 Mar	4	120	-15	306	85	0.67	0.52
RSH	Riparian Shrub	2022	21 Mar	25 Mar	4	136	-17	366	101	0.60	0.46
TSK	Tussock	2022	21 Mar	25 Mar	4	34	-18	206	14	0.77	0.63
TSK	Tussock	2023	30 Mar	13 May	44	51	-16	298	36	0.68	0.53
SHT	Shrub/Tree	2023	31 Mar	11 May	41	107	-10	329	68	0.64	0.50
SHR	Shrub	2023	31 Mar	25 Apr	25	47	-13	295	30	0.68	0.53

https://doi.org/10.5194/egusphere-2026-3835
Preprint. Discussion started: 14 July 2026

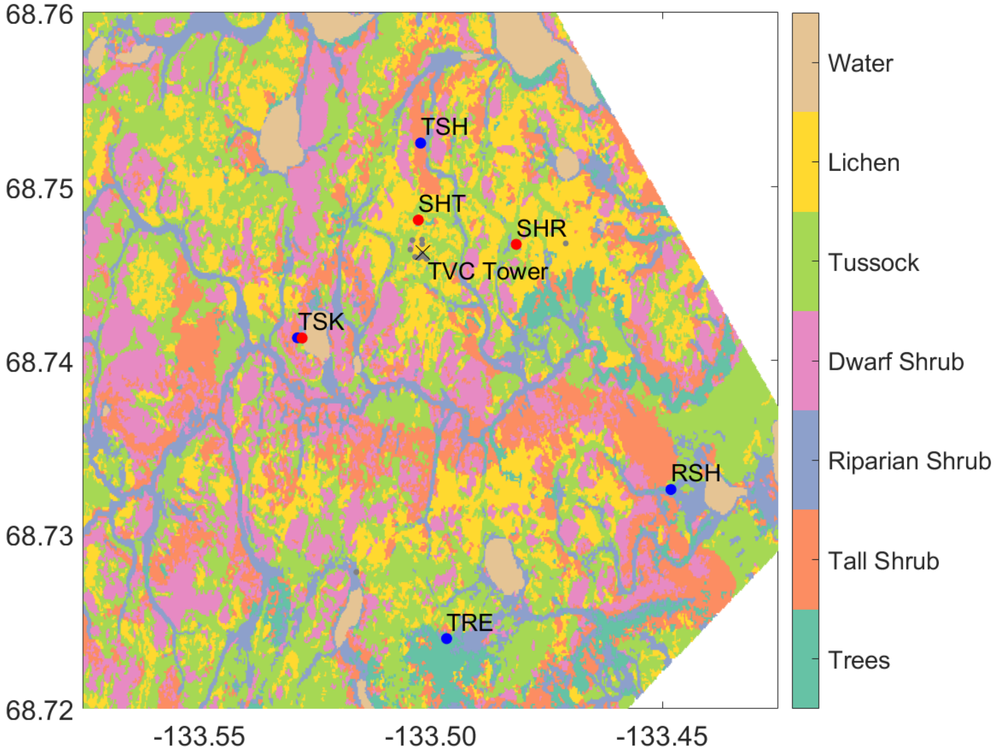

Figure 2: Vegetation types at Trail Valley Creek at 10 m × 10 m resolution (Grünberg and Boike, 2019). Locations of microsites in 2022 (blue) and 2023 (red) are shown (see Table 1 for explanation of microsite names). Meteorological measurements were made at TVC Tower (CA-TVC in AmeriFlux network; Graveline et al., 2024). Grey dots around the tower show isotope sampling locations.

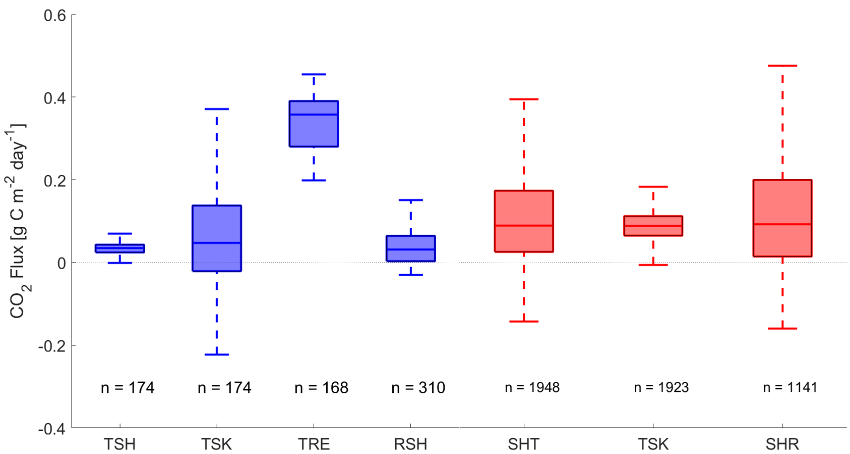

Figure 3: CO_2 fluxes measured using low-cost systems; 2022 (version 1) microsites are shown in blue and 2023 (version 2) microsites in red. Microsite names refer to the vegetation type for each location (e.g. TSK for Tussock), as given in Table 1, n denotes the number of half hourly mean flux values.

https://doi.org/10.5194/egusphere-2026-3835
Preprint. Discussion started: 14 July 2026

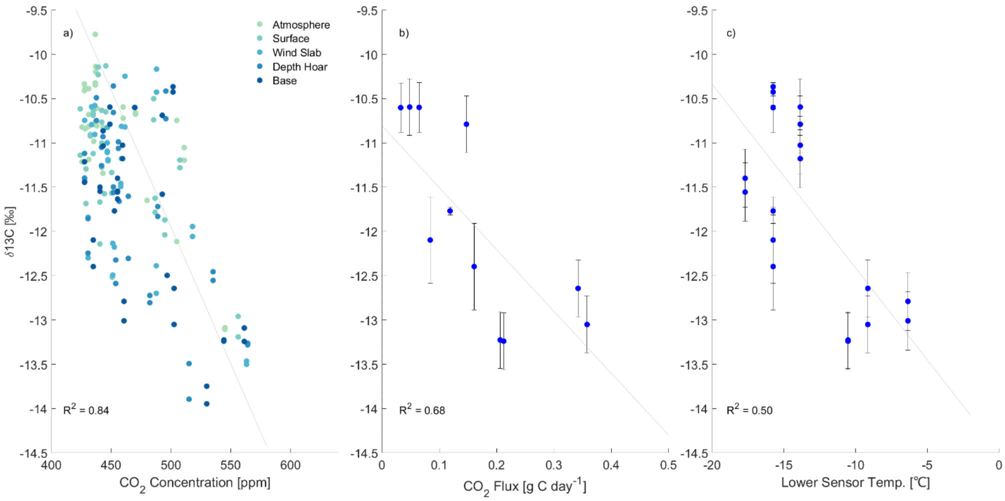

Figure 4: a) δ[13]C ratios and CO_2 concentrations from all snow profiles. Colours indicate vertical location of sample within snow profile, atmosphere includes samples measured at any height above the snowpack, surface samples are taken ≤5 cm below the air:snow interface. b) δ[13]C ratios and CO_2 fluxes (calculated from base and atmosphere IRMS CO_2 concentration measurements at each microsite). c) mean gas temperature for the total deployment from the lower sensors. R_2 values for linear regression are shown in the bottom left of each plot, plotted as a grey line. Uncertainty values for δ[13]C ratios are < 0.5 ‰. Uncertainties for CO_2 concentrations from the isotope ratio mass spectrometer (IRMS) shown in b) have a maximum value of 2.7% (or 15 ppm), but are typically <5 ppm.

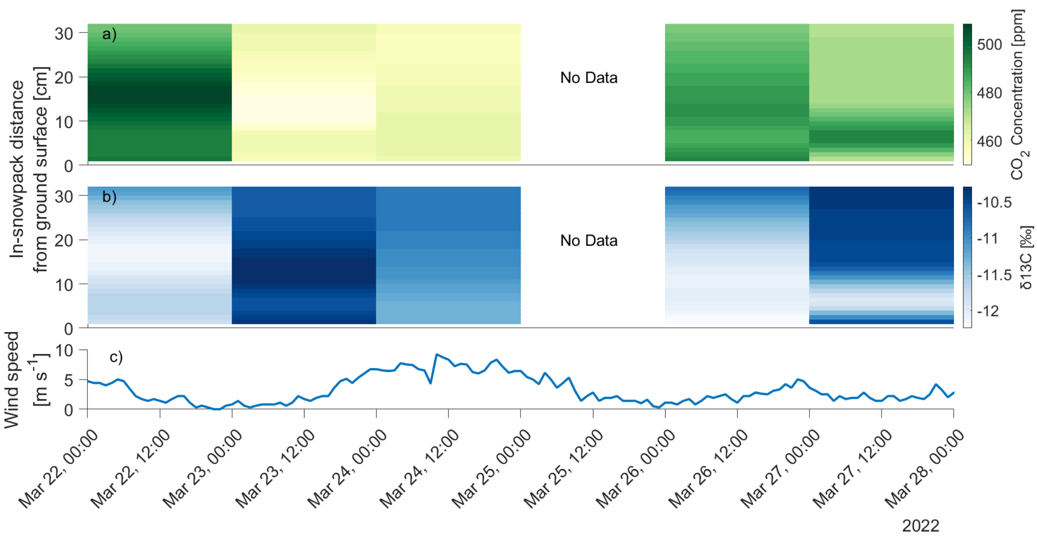

Figure 5: Daily profiles of a) CO_2 concentration (from IRMS) and b) isotopic δ[13]C signatures from an approximately 35 cm snowpack near TVC tower, interpolated to a 1 cm resolution. Darker colours represent a) higher CO_2 concentrations and b) less negative δ[13]C values.

https://doi.org/10.5194/egusphere-2026-3835
Preprint. Discussion started: 14 July 2026

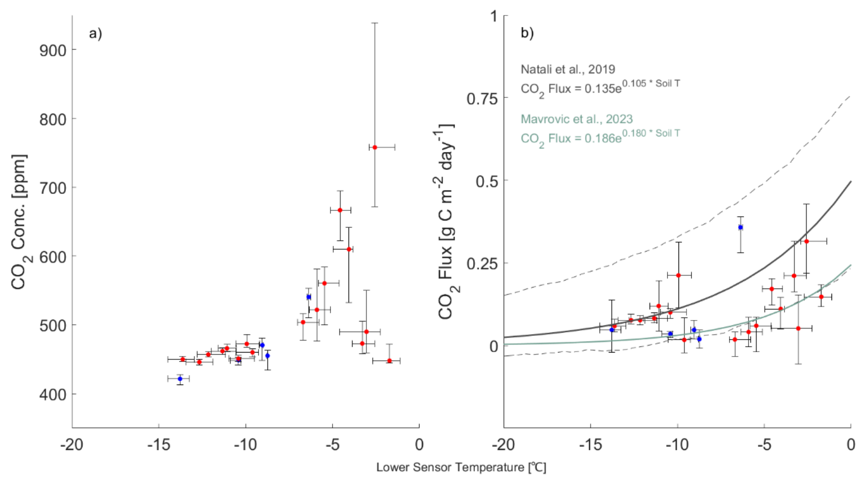

Figure 6: Weekly median gas temperatures at the base of the snowpack against; a) CO_2 concentrations at the base of the snowpack, and b) CO_2 fluxes, for both 2022 (blue) and 2023 (red) microsites. Error bars show interquartile ranges of half-hourly values. The fit of Natali et al. (2019) is shown in b), with the standard deviation of their exponential model denoted using dashed lines, and the fit of Mavrovic et al. (2023) in green.

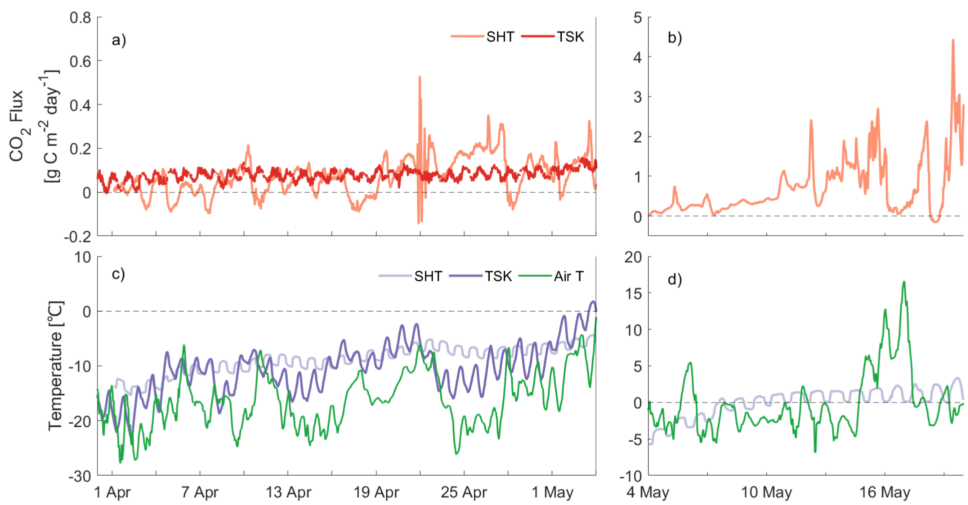

Figure 7: CO_2 flux at half-hourly resolution (a & b), and (c & d) lower sensor gas temperatures (purple; half-hourly resolution) and air temperature at the TVC Tower (green; hourly resolution) for 2023. Panels a and c show data before the zero-degree air temperature threshold is first exceeded on 4 May, note different temperature and CO_2 flux scales in panels b and d from 4 May onwards. Unlike elsewhere in the paper, panels b and d show sensor data after weekly median lower sensor temperatures exceed 0°C.

https://doi.org/10.5194/egusphere-2026-3835
Preprint. Discussion started: 14 July 2026

Appendix A – Snowpack Gas Sampling

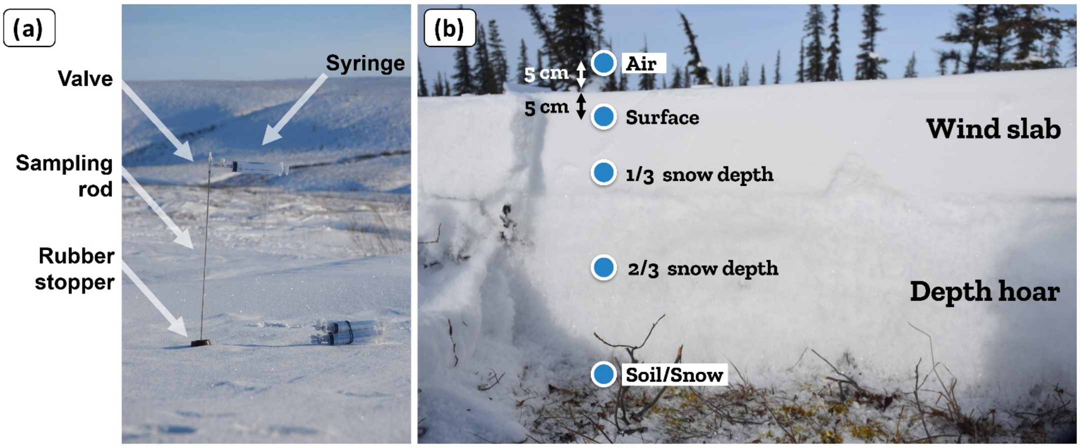

Figure A: a) Equipment set-up for snowpack gas sampling. b) Heights of snowpack gas samples within a snowpit face. Figure reproduced from Mavrovic et al. (2023).

Appendix B – Bayesian mixing model results

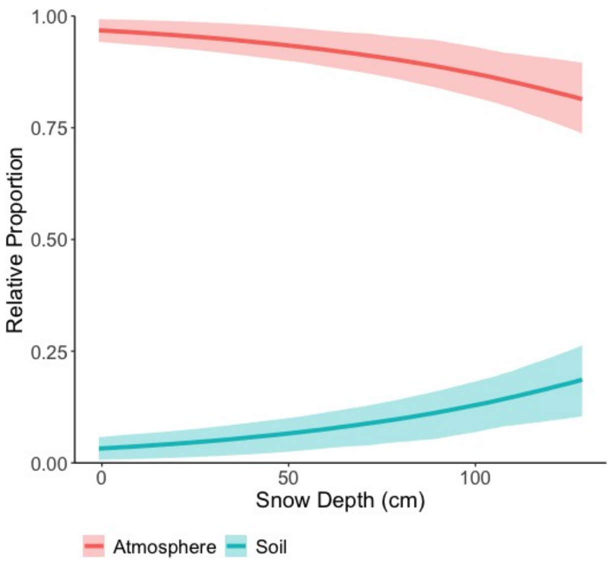

Figure B: Posterior estimate of the relative proportion of CO_2 from each source as a function of snow depth (cm). Solid line indicates the median; shading indicates the 95% confidence interval.

https://doi.org/10.5194/egusphere-2026-3835
Preprint. Discussion started: 14 July 2026

Code and Data Availability

Code to reproduce the figures within this paper is available at: https://github.com/V-Dutch/TVC_LowCostCO2Sensors
Data available at Grünberg and Boike, (2019), Tutton et al. (2026) and www.doi.org/10.6084/m9.figshare.32803616.
Data at Figshare is under embargo under the paper is accepted. A private link will be made available to reviewers.

Author Contribution

Formal analysis: VRD, PM, NR; Investigation: VRD, PM, AM; Resources (Isotope Analysis): SM; Resources (Sensor Design & Manufacture): MWK, PM; Supervision: NR, AR; Writing (Original Draft Preparation): VRD, NR. All authors were involved in reviewing and editing prior to submission.

Competing Interests

The contact author has declared that none of the authors has any competing interests.

Acknowledgements & Financial Support

The authors would like to acknowledge that this study occurred within the Inuvialuit Settlement Region of Inuit Nunangat, the traditional, ancestral and unceded lands of the Inuit people. The project was conducted with approval issued by the Aurora Research Institute (licence no. 17232). This research has been supported by the UK Natural Environment Research Council (Carbon Emissions under Arctic Snow – grant # NE/W003686/1). Victoria R. Dutch was funded by an RDF Studentship from Northumbria University and the Northern Water Futures project. Muhammad Waqas Khan was funded by the NERC CINUK grant NUNA (NE/X005658/1). Alex Mavrovic was funded by FRQNT and NSERC. Carolina Voigt was supported by the European Research Council Starting Grant COLDSPOT (no. 101163177). We would also like to thank the field teams at Trail Valley Creek in March 2022 and March 2023.

References

Ali, A. S., Zanzinger, Z., Debose, D., and Stephens, B.: Open Source Building Science Sensors (OSBSS): A low-cost Arduino-based platform for long-term indoor environmental data collection, Building and Environment, 100, 114–126, https://doi.org/10.1016/j.buildenv.2016.02.010, 2016.

Air - Diffusion Coefficients of Gases in Excess of Air: https://www.engineeringtoolbox.com/air-diffusion-coefficient-gas-mixture-temperature-d_2010.html, last access: 1 February 2023.

Arndt, K. A., Hashemi, J., Natali, S. M., Schiferl, L. D., and Virkkala, A.-M.: Recent Advances and Challenges in Monitoring and Modeling Non-Growing Season Carbon Dioxide Fluxes from the Arctic Boreal Zone, Curr Clim Change Rep, 9, 27–40, https://doi.org/10.1007/s40641-023-00190-4, 2023.

Bastviken, D., Sundgren, I., Natchimuthu, S., Reyier, H., and Gålfalk, M.: Technical Note: Cost-efficient approaches to measure carbon dioxide (CO_2) fluxes and concentrations in terrestrial and aquatic environments using mini loggers, Biogeosciences, 12, 3849–3859, https://doi.org/10.5194/bg-12-3849-2015, 2015.

Bintanja, R. and Andry, O.: Towards a rain-dominated Arctic, Nature Clim Change, 7, 263–267, https://doi.org/10.1038/nclimate3240, 2017.

Bjerke, J. W., López-Blanco, E., Tømmervik, H., Striberny, A., Davids, C., Ólafsdóttir, R., Karlsen, S. R., Sandström, P., Turunen, M., Rikkonen, T., Arneberg, M. K., Siikavuopio, S., Zinglersen, K., Lynge-Pedersen, K., Sandström, S., and Rautio, P.: Nordic boreo-arctic lands under rapid climatic change: A review of recent and future trends and extreme events, Earth-Science Reviews, 105012, https://doi.org/10.1016/j.earscirev.2024.105012, 2024.

Björkman, M. P., Morgner, E., Björk, R. G., Cooper, E. J., Elberling, B., and Klemedtsson, L.: A comparison of annual and seasonal carbon dioxide effluxes between sub-Arctic Sweden and High-Arctic Svalbard, Polar Research, 29, 75–84, https://doi.org/10.1111/j.1751-8369.2010.00150.x, 2010.

Blackstock, J. M., Covington, M. D., Perne, M., and Myre, J. M.: Monitoring Atmospheric, Soil, and Dissolved CO2 Using a Low-Cost, Arduino Monitoring Platform (CO2-LAMP): Theory, Fabrication, and Operation, Front. Earth Sci., 7, https://doi.org/10.3389/feart.2019.00313, 2019.

Boike, J., Abramov, A., Bennett, K. E., and Kutzbach, L.: Arctic permafrost, in: Encyclopedia of Soils in the Environment (Second Edition), edited by: Goss, M. J. and Oliver, M., Academic Press, Oxford, 410–418, https://doi.org/10.1016/B978-0-12-822974-3.00141-5, 2023.

Boström, B., Comstedt, D., and Ekblad, A.: Isotope fractionation and 13C enrichment in soil profiles during the decomposition of soil organic matter, Oecologia, 153, 89–98, https://doi.org/10.1007/s00442-007-0700-8, 2007.

Bowling, D. R., Massman, W. J., Schaeffer, S. M., Burns, S. P., Monson, R. K., and Williams, M. W.: Biological and physical influences on the carbon isotope content of CO2 in a subalpine forest snowpack, Niwot Ridge, Colorado, Biogeochemistry, 95, 37–59, https://doi.org/10.1007/s10533-008-9233-4, 2009.

Box, J. E., Colgan, W. T., Christensen, T. R., Schmidt, N. M., Lund, M., Parmentier, F.-J. W., Brown, R., Bhatt, U. S., Euskirchen, E. S., Romanovsky, V. E., Walsh, J. E., Overland, J. E., Wang, M., Corell, R. W., Meier, W. N., Wouters, B., Mernild, S., Mård, J., Pawlak, J., and Olsen, M. S.: Key indicators of Arctic climate change: 1971–2017, Environmental Research Letters, 14, https://doi.org/10.1088/1748-9326/aafc1b, 2019.

Bradley, J. A., Molares Moncayo, L., Gallo, G., Brusca, J., Viglezio, T., Pasotti, J., and Giovannelli, D.: Svalbard winter warming is reaching melting point, Nat Commun, 16, 6409, https://doi.org/10.1038/s41467-025-60926-8, 2025.

Bruhwiler, L., Parmentier, F.-J. W., Crill, P., Leonard, M., and Palmer, P. I.: The Arctic Carbon Cycle and Its Response to Changing Climate, Current Climate Change Reports, 7, 14–34, https://doi.org/10.1007/s40641-020-00169-5, 2021.

Byun, E., Rezanezhad, F., Fairbairn, L., Slowinski, S., Basiliko, N., Price, J. S., Quinton, W. L., Roy-Leveillee, P., Webster, K., and Van Cappellen, P.: Temperature, moisture and freeze-thaw controls on CO2 production in soil incubations from northern peatlands, Sci Rep, 11, 23219, https://doi.org/10.1038/s41598-021-02606-3, 2021.

Celis, G., Mauritz, M., Bracho, R., Salmon, V. G., Webb, E. E., Hutchings, J., Natali, S. M., Schädel, C., Crummer, K. G., and Schuur, E. A. G.: Tundra is a consistent source of CO2 at a site with progressive permafrost thaw during 6 years of chamber and eddy covariance measurements, Journal of Geophysical Research: Biogeosciences, 122, 1471–1485, https://doi.org/10.1002/2016jg003671, 2017.

Chen, S., Wang, J., Zhang, T., and Hu, Z.: Climatic, soil, and vegetation controls of the temperature sensitivity (Q10) of soil respiration across terrestrial biomes, Global Ecology and Conservation, 22, https://doi.org/10.1016/j.gecco.2020.e00955, 2020.

Christiansen, C. T., Schmidt, N. M., and Michelsen, A.: High Arctic Dry Heath CO2 Exchange During the Early Cold Season, Ecosystems, 15, 1083–1092, https://doi.org/10.1007/s10021-012-9569-4, 2012.

Clark, D. B., Mercado, L. M., Sitch, S., Jones, C. D., Gedney, N., Best, M. J., Pryor, M., Rooney, G. G., Essery, R. L. H., Blyth, E., Boucher, O., Harding, R. J., Huntingford, C., and Cox, P. M.: The Joint UK Land Environment Simulator (JULES), model description – Part 2: Carbon fluxes and vegetation dynamics, Geoscientific Model Development, 4, 701–722, https://doi.org/10.5194/gmd-4-701-2011, 2011.

Colbeck, S. C.: Model of wind pumping for layered snow, Journal of Glaciology, 43, 60–65, 1997.

Conger, S. M. and McClung, D. M.: Comparison of density cutters for snow profile observations, Journal of Glaciology, 55, 163–169, 2009.

Derksen, C., Sturm, M., Holmgren, J., Liston, G. E., Huntington, H., Silis, A., and Solie, D.: Northwest Territories and Nunavut Snow Characteristics from a Subarctic Traverse: Implications for Passive Microwave Remote Sensing, Journal of Hydrometeorology, 10, 448–463, https://doi.org/10.1175/2008jhm1074.1, 2009.

Derksen, C., Lemmetyinen, J., Toose, P., Silis, A., Pulliainen, J., and Sturm, M.: Physical properties of Arctic versus subarctic snow: Implications for high latitude passive microwave snow water equivalent retrievals, Journal of Geophysical Research: Atmospheres, 119, 7254–7270, https://doi.org/10.1002/2013jd021264, 2014.

Du, E., Zhou, Z., Li, P., Jiang, L., Hu, X., and Fang, J.: Winter soil respiration during soil-freezing process in a boreal forest in Northeast China, J Plant Ecol, 6, 349–357, https://doi.org/10.1093/jpe/rtt012, 2013.

Dutch, V. R., Rutter, N., Wake, L., Sandells, M., Derksen, C., Walker, B., Hould Gosselin, G., Sonnentag, O., Essery, R., Kelly, R., Marsh, P., King, J., and Boike, J.: Impact of measured and simulated tundra snowpack properties on heat transfer, The Cryosphere, 16, 4201–4222, https://doi.org/10.5194/tc-16-4201-2022, 2022.

Dutch, V. R., Rutter, N., Wake, L., Sonnentag, O., Hould Gosselin, G., Sandells, M., Derksen, C., Walker, B., Meyer, G., Essery, R., Kelly, R., Marsh, P., Boike, J., and Detto, M.: Simulating net ecosystem exchange under seasonal snow cover at an Arctic tundra site, Biogeosciences, 21, 825–841, https://doi.org/10.5194/bg-21-825-2024, 2024.

Ehleringer, J. R., Bowling, D. R., Flanagan, L. B., Fessenden, J., Helliker, B., Martinelli, L. A., and Ometto, J. P.: Stable Isotopes and Carbon Cycle Processes in Forests and Grasslands, Plant Biol (Stuttg), 4, 181–189, https://doi.org/10.1055/s-2002-25733, 2002.

Euskirchen, E. S., Bret-Harte, M. S., Scott, G. J., Edgar, C., and Shaver, G. R.: Seasonal patterns of carbon dioxide and water fluxes in three representative tundra ecosystems in northern Alaska, Ecosphere, 3, https://doi.org/10.1890/es11-00202.1, 2012.

Euskirchen, E. S., Bret-Harte, M. S., Shaver, G. R., Edgar, C. W., and Romanovsky, V. E.: Long-Term Release of Carbon Dioxide from Arctic Tundra Ecosystems in Alaska, Ecosystems, 20, 960–974, https://doi.org/10.1007/s10021-016-0085-9, 2016.

Fahnestock, J. T., Jones, M. H., Brooks, P. D., Walker, D. A., and Welker, J. M.: Winter and early spring CO2 efflux from tundra communities of northern Alaska, Journal of Geophysical Research: Atmospheres, 103, 29023–29027, https://doi.org/10.1029/98jd00805, 1998.

Fahnestock, J. T., Jones, M. H., and Welker, J. M.: Wintertime CO2 efflux from Arctic soils: Implications for annual carbon budgets, Global Biogeochemical Cycles, 13, 775–779, https://doi.org/10.1029/1999gb900006, 1999.

Fierz, C., Armstrong, R. L., Durand, Y., Etchevers, P., Greene, E., McClung, D. M., Nishimura, K., Satyawali, P. K., and Sokratov, S. A.: The International Classification for Seasonal Snow on the ground, 2009.

Filippa, G., Freppaz, M., Williams, M. W., Helmig, D., Liptzin, D., Seok, B., Hall, B., and Chowanski, K.: Winter and Summer Nitrous Oxide and Nitrogen Oxides Fluxes from a Seasonally Snow-Covered Subalpine Meadow at Niwot Ridge, Colorado, Biogeochemistry, 95, 131–149, 2009.

Giesse, C., Notz, D., and Baehr, J.: The Shifting Distribution of Arctic Daily Temperatures Under Global Warming, Earth's Future, 12, e2024EF004961, https://doi.org/10.1029/2024EF004961, 2024.

https://doi.org/10.5194/egusphere-2026-3835
Preprint. Discussion started: 14 July 2026

Goodrich, J. P., Oechel, W. C., Gioli, B., Moreaux, V., Murphy, P. C., Burba, G., and Zona, D.: Impact of different eddy covariance sensors, site set-up, and maintenance on the annual balance of CO2 and CH4 in the harsh Arctic environment, Agricultural and Forest Meteorology, 228–229, 239–251, https://doi.org/10.1016/j.agrformet.2016.07.008, 2016.

Graham, L. and Risk, D.: Explaining CO2 fluctuations observed in snowpacks, Biogeosciences, 15, 847–859, https://doi.org/10.5194/bg-15-847-2018, 2018.

Graveline, V., Helbig, M., Gosselin, G. H., Alcock, H., Detto, M., Walker, B., Marsh, P., and Sonnentag, O.: Surface-atmosphere energy exchanges and their effects on surface climate and atmospheric boundary layer characteristics in the forest-tundra ecotone in northwestern Canada, Agricultural and Forest Meteorology, 350, 109996, https://doi.org/10.1016/j.agrformet.2024.109996, 2024.

Grünberg, I. and Boike, J.: Vegetation map of Trail Valley Creek, Northwest Territories, Canada, https://doi.org/https://doi.org/10.1594/PANGAEA.904270, 2019.

Hanis, K. L., Tenuta, M., Amiro, B. D., and Papakyriakou, T. N.: Seasonal dynamics of methane emissions from a subarctic fen in the Hudson Bay Lowlands, Biogeosciences, 10, 4465–4479, https://doi.org/10.5194/bg-10-4465-2013, 2013.

Hould Gosselin, G., Rutter, N., Mann, P., Marsh, P., and Sonnentag, O.: Fine-scale spatial variability of winter CO_2 and CH_4 fluxes in Arctic tundra derived from snowpack gradient measurements, EGUsphere, 1–30, https://doi.org/10.5194/egusphere-2025-5637, 2025.

Jentzsch, K., Schulz, A., Pirk, N., Foken, T., Crewell, S., and Boike, J.: High Levels of CO2 Exchange During Synoptic-Scale Events Introduce Large Uncertainty Into the Arctic Carbon Budget, Geophysical Research Letters, 48, https://doi.org/10.1029/2020gl092256, 2021a.

Jentzsch, K., Boike, J., and Foken, T.: Importance of the Webb, Pearman, and Leuning (WPL) correction for the measurement of small CO_2 fluxes, Atmospheric Measurement Techniques, 14, 7291–7296, https://doi.org/10.5194/amt-14-7291-2021, 2021b.

Johnson, N., Behe, C., Danielsen, F., Krümmel, E.-M., Nickelss, S., and Pulsifer, P. L.: Community-Based Monitoring and Indigenous Knowledge in a Changing Arctic: A Review for the Sustaining Arctic Observing Networks, Inuit Circumpolar Council, Ottawa, ON, 2016.

Kade, A., Bret-Harte, M. S., Euskirchen, E. S., Edgar, C., and Fulweber, R. A.: Upscaling of CO2 fluxes from heterogeneous tundra plant communities in Arctic Alaska, Journal of Geophysical Research: Biogeosciences, 117, https://doi.org/10.1029/2012JG002065, 2012.

Kim, S.-T., Coplen, T. B., and Horita, J.: Normalization of stable isotope data for carbonate minerals: Implementation of IUPAC guidelines, Geochimica et Cosmochimica Acta, 158, 276–289, https://doi.org/10.1016/j.gca.2015.02.011, 2015.

Lawrence, D. M., Fisher, R. A., Koven, C. D., Oleson, K. W., Swenson, S. C., Bonan, G., Collier, N., Ghimire, B., Kampenhout, L., Kennedy, D., Kluzek, E., Lawrence, P. J., Li, F., Li, H., Lombardozzi, D., Riley, W. J., Sacks, W. J., Shi, M., Vertenstein, M., Wieder, W. R., Xu, C., Ali, A. A., Badger, A. M., Bisht, G., Broeke, M., Brunke, M. A., Burns, S. P., Buzan, J., Clark, M., Craig, A., Dahlin, K., Drewniak, B., Fisher, J. B., Flanner, M., Fox, A. M., Gentine, P., Hoffman, F., Keppel-Aleks, G., Knox, R., Kumar, S., Lenaerts, J., Leung, L. R., Lipscomb, W. H., Lu, Y., Pandey, A., Pelletier, J. D., Perket, J., Randerson, J. T., Ricciuto, D. M., Sanderson, B. M., Slater, A., Subin, Z. M., Tang, J., Thomas, R. Q., Val Martin, M., and Zeng, X.: The Community Land Model Version 5: Description of New Features, Benchmarking, and Impact of Forcing Uncertainty, Journal of Advances in Modeling Earth Systems, 11, 4245–4287, https://doi.org/10.1029/2018ms001583, 2019.

Levitt, N. P.: Sample matrix effects on measured carbon and oxygen isotope ratios during continuous-flow isotope-ratio mass spectrometry, Rapid Commun Mass Spectrom, 28, 2259–74, https://doi.org/10.1002/rcm.7019, 2014.

Levy, P., Clement, R., Cowan, N., Keane, B., Myrgiotis, V., van Oijen, M., Smallman, T. L., Toet, S., and Williams, M.: Challenges in Scaling Up Greenhouse Gas Fluxes: Experience From the UK Greenhouse Gas Emissions and Feedbacks Program, Journal of Geophysical Research: Biogeosciences, 127, e2021JG006743, https://doi.org/10.1029/2021JG006743, 2022.

Lupascu, M., Czimczik, C. I., Welker, M. C., Ziolkowski, L. A., Cooper, E. J., and Welker, J. M.: Winter Ecosystem Respiration and Sources of CO2 From the High Arctic Tundra of Svalbard: Response to a Deeper Snow Experiment, Journal of Geophysical Research: Biogeosciences, 123, 2627–2642, https://doi.org/10.1029/2018jg004396, 2018.

Maina, F. Z. and Kumar, S. V.: Global patterns of rain-on-snow and its impacts on runoff from past to future projections, Nat Commun, 16, 4731, https://doi.org/10.1038/s41467-025-59855-3, 2025.

Mast, M. A., Wickland, K. P., Striegl, R. T., and Clow, D. W.: Winter fluxes of CO2 and CH4 from subalpine soils in Rocky Mountain National Park, Colorado, Global Biogeochemical Cycles, 12, 607–620, https://doi.org/10.1029/98gb02313, 1998.

Mavrovic, A., Sonnentag, O., Lemmetyinen, J., Voigt, C., Rutter, N., Mann, P., Sylvain, J.-D., and Roy, A.: Environmental controls of winter soil carbon dioxide fluxes in boreal and tundra environments, Biogeosciences, 20, 5087–5108, https://doi.org/10.5194/bg-20-5087-2023, 2023.

Mazzola, V., Perks, M. P., Smith, J., Yeluripati, J., and Xenakis, G.: Assessing soil carbon dioxide and methane fluxes from a Scots pine raised bog-edge-woodland, Journal of Environmental Management, 302, 114061, https://doi.org/10.1016/j.jenvman.2021.114061, 2022.

Muhr, J., Borken, W., and Matzner, E.: Effects of soil frost on soil respiration and its radiocarbon signature in a Norway spruce forest soil, Global Change Biology, 15, 782–793, https://doi.org/10.1111/j.1365-2486.2008.01695.x, 2009.

Natali, S. M., Watts, J. D., Rogers, B. M., Potter, S., Ludwig, S. M., Selbmann, A.-K., Sullivan, P. F., Abbott, B. W., Arndt, K. A., Birch, L., Björkman, M. P., Bloom, A. A., Celis, G., Christensen, T. R., Christiansen, C. T., Commane, R., Cooper, E. J., Crill, P., Czimczik, C., Davydov, S., Du, J., Egan, J. E., Elberling, B., Euskirchen, E. S., Friborg, T., Genet, H., Göckede, M., Goodrich, J. P., Grogan, P., Helbig, M., Jafarov, E. E., Jastrow, J. D., Kalhori, A. A. M., Kim, Y., Kimball, J. S., Kutzbach, L., Lara, M. J., Larsen, K. S., Lee, B.-Y., Liu, Z., Loranty, M. M., Lund, M., Lupascu, M., Madani, N., Malhotra, A., Matamala, R., McFarland, J., McGuire, A. D., Michelsen, A., Minions, C., Oechel, W. C., Olefeldt, D., Parmentier, F.-J. W., Pirk, N., Poulter, B., Quinton, W., Rezanezhad, F., Risk, D., Sachs, T., Schaefer, K., Schmidt, N. M., Schuur, E. A. G., Semenchuk, P. R., Shaver, G., Sonnentag, O., Starr, G., Treat, C. C., Waldrop, M. P., Wang, Y., Welker, J., Wille, C., Xu, X., Zhang, Z., Zhuang, Q., and Zona, D.: Large loss of CO2 in winter observed across the northern permafrost region, Nature Climate Change, 9, 852–857, https://doi.org/10.1038/s41558-019-0592-8, 2019.

Nickerson, N. and Risk, D.: Physical controls on the isotopic composition of soil-respired CO2, Journal of Geophysical Research, 114, https://doi.org/10.1029/2008jg000766, 2009.

Noguchi, K., Matsuura, Y., Morishita, T., Toriyama, J., and Kim, Y.: Fine Root Growth of Black Spruce Trees and Understory Plants in a Permafrost Forest Along a North-Facing Slope in Interior Alaska, Front. Plant Sci., 12, https://doi.org/10.3389/fpls.2021.769710, 2021.

Oechel, W. C., Laskowski, C. A., Burba, G., Gioli, B., and Kalhori, A. A. M.: Annual patterns and budget of CO2 flux in an Arctic tussock tundra ecosystem, Journal of Geophysical Research: Biogeosciences, 119, 323–339, https://doi.org/10.1002/2013jg002431, 2014.

Oyola, P., Carbone, S., Timonen, H., Torkmahalleh, M., and Lindén, J.: Editorial: Rise of Low-Cost Sensors and Citizen Science in Air Quality Studies, Front. Environ. Sci., 10, https://doi.org/10.3389/fenvs.2022.868543, 2022.

Pallandt, M., Kumar, J., Mauritz, M., Schuur, E., Virkkala, A.-M., Celis, G., Hoffman, F., and Göckede, M.: Representativeness assessment of the pan-Arctic eddy-covariance site network, and optimized future enhancements, Biogeosciences Discussions, https://doi.org/10.5194/bg-2021-133, 2021.

Paré, M. C. and Bedard-Haughn, A.: Soil organic matter quality influences mineralization and GHG emissions in cryosols: a field-based study of sub- to high Arctic, Global Change Biology, 19, 1126–1140, https://doi.org/10.1111/gcb.12125, 2013.

Pedron, S. A., Welker, J. M., Euskirchen, E. S., Klein, E. S., Walker, J. C., Xu, X., and Czimczik, C. I.: Closing the Winter Gap—Year-Round Measurements of Soil CO2 Emission Sources in Arctic Tundra, Geophysical Research Letters, 49, https://doi.org/10.1029/2021gl097347, 2022.

Pedron, S. A., Jespersen, R. G., Xu, X., Khazindar, Y., Welker, J. M., and Czimczik, C. I.: More Snow Accelerates Legacy Carbon Emissions From Arctic Permafrost, AGU Advances, 4, e2023AV000942, https://doi.org/10.1029/2023AV000942, 2023.

Pino, H., Pastor, V., Grimalt-Álvaro, C., and López, V.: Measuring CO2 with an Arduino: Creating a Low-Cost, Pocket-Sized Device with Flexible Applications That Yields Benefits for Students and Schools, J. Chem. Educ., 96, 377–381, https://doi.org/10.1021/acs.jchemed.8b00473, 2019.

Pirk, N., Tamstorf, M. P., Lund, M., Mastepanov, M., Pedersen, S. H., Mylius, M. R., Parmentier, F.-J. W., Christiansen, H. H., and Christensen, T. R.: Snowpack fluxes of methane and carbon dioxide from high Arctic tundra, Journal of Geophysical Research: Biogeosciences, 121, 2886–2900, https://doi.org/10.1002/2016jg003486, 2016.

Pirk, N., Sievers, J., Mertes, J., Parmentier, F.-J. W., Mastepanov, M., and Christensen, T. R.: Spatial variability of CO2 uptake in polygonal tundra: assessing low-frequency disturbances in eddy covariance flux estimates, Biogeosciences, 14, 3157–3169, https://doi.org/10.5194/bg-14-3157-2017, 2017.

Pirk, N., Aalstad, K., Mannerfelt, E. S., Clayer, F., de Wit, H., Christiansen, C. T., Althuizen, I., Lee, H., and Westermann, S.: Disaggregating the Carbon Exchange of Degrading Permafrost Peatlands Using Bayesian Deep Learning, Geophysical Research Letters, 51, e2024GL109283, https://doi.org/10.1029/2024GL109283, 2024.

Previdi, M., Smith, K. L., and Polvani, L. M.: Arctic amplification of climate change: a review of underlying mechanisms, Environmental Research Letters, 16, https://doi.org/10.1088/1748-9326/ac1c29, 2021.

Proksch, M., Löwe, H., and Schneebeli, M.: Density, specific surface area, and correlation length of snow measured by high-resolution penetrometry, Journal of Geophysical Research: Earth Surface, 120, 346–362, https://doi.org/10.1002/2014jf003266, 2015.

Rafat, A., Rezanezhad, F., Quinton, W. L., Humphreys, E. R., Webster, K., and Van Cappellen, P.: Non-growing season carbon emissions in a northern peatland are projected to increase under global warming, Communications Earth & Environment, 2, https://doi.org/10.1038/s43247-021-00184-w, 2021.

Rains, F. A., Stoy, P. C., Welch, C. M., Montagne, C., and McGlynn, B. L.: A Comparison of Methods Reveals that Enhanced Diffusion Helps Explain Cold-Season Soil CO2 Efflux in a Lodgepole Pine Ecosystem, Cold Regions Science and Technology, 121, 16–24, https://doi.org/10.1016/j.coldregions.2015.10.003, 2016.

Rantanen, M., Karpechko, A. Y., Lipponen, A., Nordling, K., Hyvärinen, O., Ruosteenoja, K., Vihma, T., and Laaksonen, A.: The Arctic has warmed nearly four times faster than the globe since 1979, Communications Earth & Environment, 3, https://doi.org/10.1038/s43247-022-00498-3, 2022.

Raz-Yaseef, N., Torn, M. S., Wu, Y., Billesbach, D. P., Liljedahl, A. K., Kneafsey, T. J., Romanovsky, V. E., Cook, D. R., and Wullschleger, S. D.: Large CO2 and CH4 emissions from polygonal tundra during spring thaw in northern Alaska, Geophysical Research Letters, 44, 504–513, https://doi.org/10.1002/2016gl071220, 2017.

Reivanth, K., Priya, A., and Nataraj, D.: A Low-Cost Arduino and Python Based Gas Sensing Setup: Bridging Theory and Practice in Educational Environments, J. Chem. Educ., 101, 5361–5368, https://doi.org/10.1021/acs.jchemed.4c00981, 2024.

Rooney, E. C., Bailey, V. L., Patel, K. F., Dragila, M., Battu, A. K., Buchko, A. C., Gallo, A. C., Hatten, J., Possinger, A. R., Qafoku, O., Reno, Loren. R., SanClements, M., Varga, T., and Lybrand, R. A.: Soil pore network response to freeze-thaw cycles in permafrost aggregates, Geoderma, 411, 115674, https://doi.org/10.1016/j.geoderma.2021.115674, 2022.

Saccardi, B. E., Dere, A. L., Goodwell, A. E., Druhan, J., Welp, L. R., Blair, N. E., Bauer, E., Haken, J., Jimenez-Castaneda, M. E., Filley, T., Frantal, I., and Kumar, P.: A low-power, low-cost, chamber-based CO2 sensor, Front. Water, 7, https://doi.org/10.3389/frwa.2025.1638540, 2025.

Schimel, J. P., Bilbrough, C., and Welker, J. M.: Increased snow depth affects microbial activity and nitrogen mineralization in two Arctic tundra communities, Soil Biology and Biochemistry, 36, 217–227, https://doi.org/10.1016/j.soilbio.2003.09.008, 2004.

Schuur, E. A., McGuire, A. D., Schadel, C., Grosse, G., Harden, J. W., Hayes, D. J., Hugelius, G., Koven, C. D., Kuhry, P., Lawrence, D. M., Natali, S. M., Olefeldt, D., Romanovsky, V. E., Schaefer, K., Turetsky, M. R., Treat, C. C., and Vonk, J. E.: Climate change and the permafrost carbon feedback, Nature, 520, 171–9, https://doi.org/10.1038/nature14338, 2015.

Schuur, E. A. G., Abbot, B. W., Commane, R., Ernakovich, J., Euskirchen, Eugenie, E. S., Hugelius, G., Grosse, G., Jones, M., Koven, C., Leshyk, V., Lawrence, D., Loranty, M. M., Mauritz, M., Olefeldt, D., Natali, S., Rodenhizer, H., Salmon, V., Schädel, C., Strauss, J., Treat, C., and Turetsky, M.: Permafrost and Climate Change: Carbon Cycle Feedbacks From the Warming Arctic, Annual Review of Environment and Resources, 47, 343–371, 2022.

Seok, B., Helmig, D., Williams, M. W., Liptzin, D., Chowanski, K., and Hueber, J.: An automated system for continuous measurements of trace gas fluxes through snow: an evaluation of the gas diffusion method at a subalpine forest site, Niwot Ridge, Colorado, Biogeochemistry, 95, 95–113, https://doi.org/10.1007/s10533-009-9302-3, 2009.

Skrzypek, G., Allison, C. E., Böhlke, J. K., Bontempo, L., Brewer, P., Camin, F., Carter, J. F., Chartrand, M. M. G., Coplen, T. B., Gröning, M., Hélie, J.-F., Esquivel-Hernández, G., Kraft, R. A., Magdas, D. A., Mann, J. L., Meija, J., Meijer, H. A. J., Moossen, H., Ogrinc, N., Perini, M., Possolo, A., Rogers, K. M., Schimmelmann, A., Shemesh, A., Soto, D. X., Thomas, F., Wielgosz, R., Winchester, M. R., Yan, Z., and Dunn, P. J. H.: Minimum requirements for publishing hydrogen, carbon, nitrogen, oxygen and sulfur stable-isotope delta results (IUPAC Technical Report), Pure and Applied Chemistry, 0, https://doi.org/10.1515/pac-2021-1108, 2022.

Slater, A. G., Lawrence, D. M., and Koven, C. D.: Process-level model evaluation: a snow and heat transfer metric, The Cryosphere, 11, 989–996, https://doi.org/10.5194/tc-11-989-2017, 2017.

Sommerfeld, R. A., Mosier, A. R., and Musselman, R. C.: CO2, CH4 and N2O flux through a Wyoming snowpack and implications for global budgets, Nature, 361, 140–142, 1993.

Spötl, C. and Vennemann, T. W.: Continuous-flow isotope ratio mass spectrometric analysis of carbonate minerals, Rapid Commun Mass Spectrom, 17, 1004–6, https://doi.org/10.1002/rcm.1010, 2003.

Stock, B. C. and Semmens, B. X.: MixSIAR GUI User Manual. Version 3.1, https://doi.org/10.5281/zenodo.1209993, 2016.

Stock, B. C., Jackson, A. L., Ward, E. J., Parnell, A. C., Phillips, D. L., and Semmens, B. X.: Analyzing mixing systems using a new generation of Bayesian tracer mixing models, PeerJ, 6, e5096, https://doi.org/10.7717/peerj.5096, 2018.

Tao, J., Zhu, Q., Riley, W. J., and Neumann, R. B.: Improved ELMv1-ECA simulations of zero-curtain periods and cold-season CH4 and CO2 emissions at Alaskan Arctic tundra sites, The Cryosphere, 15, 5281–5307, https://doi.org/10.5194/tc-15-5281-2021, 2021.

Thanh Duc, N., Silverstein, S., Wik, M., Crill, P., Bastviken, D., and Varner, R. K.: Technical note: Greenhouse gas flux studies: an automated online system for gas emission measurements in aquatic environments, Hydrology and Earth System Sciences, 24, 3417–3430, https://doi.org/10.5194/hess-24-3417-2020, 2020.

Tu, K. and Dawson, T.: Partitioning Ecosystem Respriration using Stable Carbon Isotope Analysis of CO2, 125–152, 2005.

Tutton, R., Dakin, B., Essery, R., Griffith, J., Hould-Gosselin, G., Marsh, P., Sonnentag, O., Thorne, R., and Walker, B.: A hydrometeorological dataset from the taiga-tundra ecotone in the western Canadian Arctic: Trail Valley Creek, Northwest Territories (4.0), https://doi.org/10.5683/SP3/BXV4DE, 2026.

Virkkala, A.-M., Virtanen, T., Lehtonen, A., Rinne, J., and Luoto, M.: The current state of CO2 flux chamber studies in the Arctic tundra: A review, Progress in Physical Geography: Earth and Environment, 42, 162–184, https://doi.org/10.1177/0309133317745784, 2018.

Virkkala, A.-M., Natali, S. M., Rogers, B. M., Watts, J. D., Savage, K., Connon, S. J., Mauritz, M., Schuur, E. A. G., Peter, D., Minions, C., Nojeim, J., Commane, R., Emmerton, C. A., Goeckede, M., Helbig, M., Holl, D., Iwata, H., Kobayashi, H., Kolari, P., López-Blanco, E., Marushchak, M. E., Mastepanov, M., Merbold, L., Parmentier, F.-J. W., Peichl, M., Sachs, T., Sonnentag, O., Ueyama, M., Voigt, C., Aurela, M., Boike, J., Celis, G., Chae, N., Christensen, T. R., Bret-Harte, M. S., Dengel, S., Dolman, H., Edgar, C. W., Elberling, B., Euskirchen, E., Grelle, A., Hatakka, J., Humphreys, E., Järveoja, J., Kotani, A., Kutzbach, L., Laurila, T., Lohila, A., Mammarella, I., Matsuura, Y., Meyer, G., Nilsson, M. B., Oberbauer, S. F., Park, S.-J., Petrov, R., Prokushkin, A. S., Schulze, C., St. Louis, V. L., Tuittila, E.-S., Tuovinen, J.-P., Quinton, W., Varlagin, A., Zona, D., and Zyryanov, V. I.: The ABCflux database: Arctic–boreal CO_2 flux observations and ancillary information aggregated to monthly time steps across terrestrial ecosystems, Earth System Science Data, 14, 179–208, https://doi.org/10.5194/essd-14-179-2022, 2022.

Webb, E. E., Schuur, E. A. G., Natali, S. M., Oken, K. L., Bracho, R., Krapek, J. P., Risk, D., and Nickerson, N. R.: Increased wintertime CO2 loss as a result of sustained tundra warming, Journal of Geophysical Research: Biogeosciences, 121, 249–265, https://doi.org/10.1002/2014jg002795, 2016.

Webb, E. K., Pearman, G. I., and Leuning, R.: Correction of flux measurements for density effects due to heat and water vapour transfer, Quarterly Journal of the Royal Meteorological Society, 106, 85–100, 1980.

Welker, J. M., Fahnestock, J. T., and Jones, M. H.: Annual CO2 flux in dry and moist arctic tundra: field responses to increases in summer temperatures and winter snow depth, 2000.

Wilcox, E. J., Keim, D., de Jong, T., Walker, B., Sonnentag, O., Sniderhan, A. E., Mann, P., and Marsh, P.: Tundra shrub expansion may amplify permafrost thaw by advancing snowmelt timing, Arctic Science, 5, 202–217, https://doi.org/10.1139/as-2018-0028, 2019.

Yamanouchi, T. and Takata, K.: Rapid change of the Arctic climate system and its global influences - Overview of GRENE Arctic climate change research project (2011–2016), Polar Science, 25, 100548, https://doi.org/10.1016/j.polar.2020.100548, 2020.

https://doi.org/10.5194/egusphere-2026-3835
Preprint. Discussion started: 14 July 2026

Zhu, X., Di, D., Ma, M., and Shi, W.: Stable Isotopes in Greenhouse Gases from Soil: A Review of Theory and Application, Atmosphere, 10, https://doi.org/10.3390/atmos10070377, 2019.

Zona, D., Gioli, B., Commane, R., Lindaas, J., Wofsy, S. C., Miller, C. E., Dinardo, S. J., Dengel, S., Sweeney, C., Karion, A., Chang, R. Y., Henderson, J. M., Murphy, P. C., Goodrich, J. P., Moreaux, V., Liljedahl, A., Watts, J. D., Kimball, J. S., Lipson, D. A., and Oechel, W. C.: Cold season emissions dominate the Arctic tundra methane budget, Proc Natl Acad Sci U S A, 113, 40–5, https://doi.org/10.1073/pnas.1516017113, 2016.